



Obrabotka metallov -

Metal Working and Material Science











Journal homepage: http://journals.nstu.ru/obrabotka_metallov



Modal analysis of various grinding wheel types for the evaluation of their integral elastic parameters

Aleksandr Zhukov^{a,*}, Dmitrii Ardashev^b, Victor Batuev^c, Victor Kulygin^d, Egor Schuleshko^e

South Ural State University, 76 Prospekt Lenina, Chelyabinsk, 454080, Russian Federation

^a  <https://orcid.org/0000-0002-9328-7148>,  zhukovas@susu.ru; ^b  <https://orcid.org/0000-0002-8134-2525>,  ardashevdy@susu.ru;
^c  <https://orcid.org/0000-0001-9969-4310>,  batuevvv@susu.ru; ^d  <https://orcid.org/0009-0000-8509-1420>,  kulyginvl@susu.ru;
^e  <https://orcid.org/0000-0002-5709-4285>,  schuleshko21@mail.ru

ARTICLE INFO

Article history:

Received: 04 May 2025

Revised: 25 May 2025

Accepted: 05 June 2025

Available online: 15 September 2025

Keywords:

Grinding
 Grinding wheel
 Grinding wheel natural vibrations
 Grinding wheel integral elastic indices
 Modal analysis
 Participation factor
 Spectral composition
 Natural vibrations frequency
 Computer modelling
 COMSOL Multiphysics
 Finite element analysis

Funding

The study was funded by the Russian Science Foundation grant No. 25-29-20029, <https://rscf.ru/en/project/25-29-20029/>

ABSTRACT

Introduction. In developing a mathematical model for the sound pressure generated by the grinding process, it became necessary to determine the actual values of the integral elastic parameters of grinding wheels to use as inputs in the model. This will expand the applicability of the model and maximize its practical utility. This paper describes an approach to determining *Poisson's* ratios and *Young's* moduli for grinding wheels with different characteristics. The elastic properties of the tool are the **subject** of this study. The **purpose** is to establish the relationship between actual values of integral elastic parameters and grinding wheel characteristics via modal analysis. The **research method** combines experimental investigation of natural frequency spectra and modal analysis, implemented via the finite element method in specialized software. Additionally, regression analysis is employed to derive empirical dependencies of the integral elastic parameters of grinding wheels on abrasive grain size and hardness. **Results and discussion.** The main result of this work is the determination of the actual values of *Poisson's* ratios and *Young's* moduli for grinding wheels with the studied characteristics. The selection of grinding wheel characteristics allowed for the investigation of the influence of abrasive grain size and hardness on its integral elastic properties. The development of a mathematical model for sound pressure generated by the grinding process, along with a methodology for predicting the service life of grinding wheels based on this model, will improve grinding operation efficiency by reducing the machine-setting time, increasing processing time, reducing consumption of manufacturing resources, and optimizing tool lifespan utilization.

For citation: Zhukov A.S., Ardashev D.V., Batuev V.V., Kulygin V.L., Schuleshko E.I. Modal analysis of various grinding wheel types for the evaluation of their integral elastic parameters. *Obrabotka metallov (tekhnologiya, oborudovanie, instrumenty) = Metal Working and Material Science*, 2025, vol. 27, no. 3, pp. 71–86. DOI: 10.17212/1994-6309-2025-27.3-71-86. (In Russian).

Introduction

Predicting the life of a grinding wheel (*GW*) by means of the indirect acoustic criterion naturally implies the need to study its dynamic characteristics. The development of a model for the sound pressure generated by the grinding process requires the values of the elastic moduli of the grinding wheel to correctly calculate the modes and frequencies of the natural vibrations which are the source of the acoustic field. According to

* Corresponding author

Zhukov Aleksandr S., Ph.D. (Engineering) student
 South Ural State University,
 76 Prospekt Lenina,
 454080, Chelyabinsk, Russian Federation
 Tel.: +7 351 272-32-94, e-mail: zhukovas@susu.ru

the characteristics of such a field, it is possible to predict many output parameters of the grinding process over time: cutting forces, machining quality parameters [1, 2] (roughness, shape deviations of the workpiece, presence of burns, etc.), and stiffness of the technological system. The sequence of manifestation of natural vibration modes of the grinding wheel, inseparably connected with its elastic parameters, determines the nature of the acoustic response of the system during operation, as well as the way it will react to external excitation during grinding.

Modal analysis is a powerful method for determining the dynamic characteristics of a mechanical system. In mechanical engineering, this method is used to solve a wide range of problems, from the design and optimization of machine structures, mechanisms, and parts, to the diagnosis and monitoring of equipment condition. The growing need to improve the design of modern metal-cutting machines and tools with respect to vibration resistance, increasing their reliability and rigidity, has led to the emergence of new and effective applications of modal analysis. In [3–8], parametric optimization of both the design of individual elements of machine tools (spindles, beds, etc.) and complex machine tool assemblies is carried out. In particular, designs of numerically controlled machine tools and multi-axis high-precision machine tools are often optimized by means of modal analysis. In [9–13], cutting tools are designed using modal analysis, and existing designs of turning tools, drills, and milling cutters are improved according to criteria of vibration resistance and enhancement of dynamic balance during machining. Calculating the eigenmodes and vibration frequencies of systems whose operation is associated with dynamic vibration loads is necessary at the design, testing, or modernization stages, regardless of the magnitude of the loads. If the system's operating mode leads to vibrations at the resonance frequency, the design is modified to prevent emergency situations.

The complexity and multi-component structure of a grinding wheel make it difficult to determine its elasticity parameters, which are necessary for calculating its natural vibrations. The elastic parameters of abrasive tools are poorly represented in technical literature. There is no systematization, and no correspondence has been established between these parameters and the characteristics of grinding wheels. Reference books do not provide values for the elastic properties of abrasive tools, such as *Poisson's* ratio and *Young's* modulus. Only isolated experimental references for grinding wheels with specific characteristics can be found.

The variety of existing and emerging grinding wheel formulations is extremely large. Depending on the characteristics of the grinding wheel, the proportions of its components (abrasive, bond, and pores) and their properties vary considerably [14]. Exact calculations of the elastic parameters of grinding wheels are extremely laborious, as they require consideration of the properties of each component and how they interact with each other. To simplify the process, modal analysis is proposed to evaluate the elastic properties of the system as a whole without detailing the components.

The **objective of this study** is to determine how the actual values of integral elastic indices depend on grinding wheel characteristics using modal analysis. To achieve this goal, the following tasks must be completed:

- 1) conduct an experimental study of the frequencies of natural vibrations of grinding wheels with different characteristics;
- 2) calculate the natural frequencies and mode shapes of grinding wheels for various combinations of elastic and geometric parameters using specialized software and the finite element method;
- 3) compare and correlate the experimental and calculated natural frequencies of the grinding wheels.
- 4) determine the actual values of *Poisson's* ratio and *Young's* modulus for all investigated grinding wheels.

Methods

Table 1 shows the list of grinding wheel characteristics included in the study of integral elastic performance.

The grinding wheels were selected for this study to investigate how changes in granularity, hardness, and abrasive material affect the integral elastic properties of the tool (Fig. 1).

Table 1

Grinding wheels characteristics according to *GOST R 52781-2007*

<i>GW</i> No.	<i>GW</i> dimensions <i>D</i> × <i>H</i> × <i>d</i> , mm	Abrasive material	Grit	Hardness
1	600×50×305	25 <i>A</i>	<i>F36</i>	<i>L</i>
2			<i>F46</i>	
3			<i>F60</i>	
4			<i>F80</i>	
5			<i>F120</i>	
6			<i>F60</i>	<i>N</i>
7				<i>P</i>
8	<i>S</i>			
9	<i>L</i>			
10		600×50×305	<i>14A</i>	
		<i>64C</i>		
11	600×40×305	<i>92A</i>		

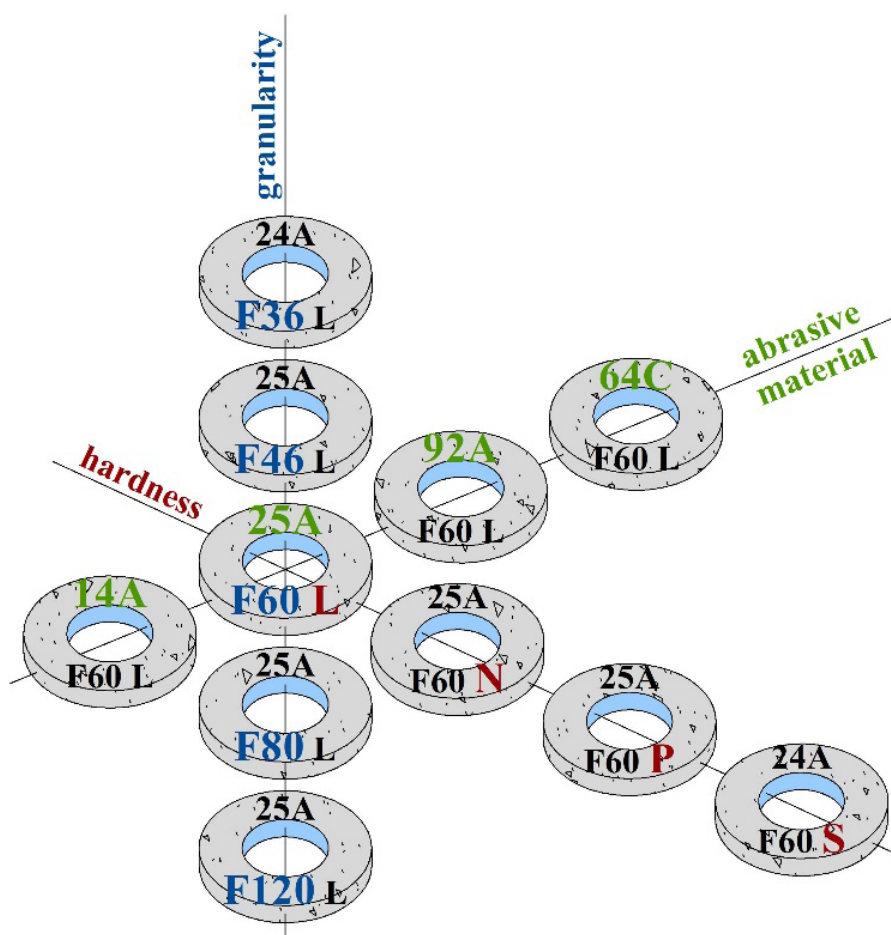


Fig. 1. Grinding wheels under study

The effect of grain size variation on the elastic properties of grinding wheels No. 1, No. 2, No. 3, No. 4, and No. 5 was studied. The grain size ranged from F36 to F120 (H50 to H10 according to *GOST 2424-84*), with the average grain size ranging from 0.5 to 0.11 mm. Other properties remained unchanged.

The influence of changes in hardness on the elastic properties of grinding wheels No. 3, No. 6, No. 7, and No. 8 was studied. The hardness varied from *L* to *S* (*CM2* to *T2* according to *GOST 2424-84*). All other formulation characteristics remained unchanged.

To study the influence of different abrasives on the elastic properties of grinding wheels, wheels No. 3, No. 9, No. 10, and No. 11 were considered:

- 25A white aluminum oxide with 99 % $\alpha\text{-Al}_2\text{O}_3$ content. It is used for finishing and profile grinding of hardened steels, as well as sharpening of high-speed tools;
- 14A normal electrocorundum with 93 % $\alpha\text{-Al}_2\text{O}_3$ content. It is used for rough grinding;
- 92A chromotitanium electrocorundum with 60–75 % $\alpha\text{-Al}_2\text{O}_3$ content. It is used for grinding hardened steels, machining with large metal removal, and rough grinding;
- 64C green silicon carbide with 96–97 % SiC content. It is used for final sharpening and finishing of carbide tools, honing, and superfinishing [14, 15].

The structure of the considered grinding wheels is medium (structure numbers 5, 6, and 7), and the bond is ceramic.

Experimental study of natural vibrations of grinding wheels

A full-scale experiment was conducted to record the spectrum of natural frequencies of grinding wheel vibrations. The natural oscillations of the grinding wheel were excited by impact, as shown in Fig. 2. The acoustic signal generated by the wheel's natural vibrations was recorded using the *NFM-2* (natural frequency meter) employing a non-contact method. The grinding wheel (*GW*) was mounted vertically on a carriage. The *ICHSK-2* microphone, which serves as the device's sensitive element, was positioned at an angle of $45^\circ \pm 15^\circ$ relative to the diameter passing through the grinding wheel's support point. A minimum clearance between the cylindrical surface of the grinding wheel and the microphone must be maintained; contact with the surface is not permitted. The striker (hammer) impacts the grinding wheel at an angle of $45^\circ \pm 15^\circ$ relative to the diameter passing through the support point of the grinding wheel, symmetrical to the microphone's position. The striker impacts the cylindrical surface of the tested bearing directed toward its center. The force and area of impact are insignificant since the study focuses on the frequencies, not the amplitudes, of natural vibrations.

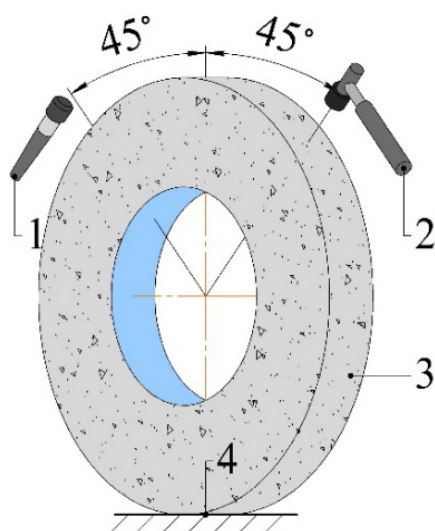


Fig. 2. Scheme of measuring frequencies of *GW* natural vibrations:

1 – microphone, 2 – hammer, 3 – grinding wheel under study, 4 – base

When setting up the device, it is necessary to specify:

- type of product – abrasives / blades / other products;
- type of abrasive – 14A / 25A / 92A / 64C;
- type of bond – bakelite / vulcanite / ceramic;
- geometric shape and dimensions of the grit (shape coefficient);
- density of the ball;
- frequency range of measurements.

The experiment involved 10 measurements of the eigenfrequencies of each grinding wheel. Then, the average spectral composition of the natural frequencies of each grinding wheel was determined. Fig. 3 shows an example of a spectrogram of ten measurements of natural frequencies of *GW* 1 600×50×305 25A F60 L 7 V 50 2kl *GOST R 52781-2007* – grinding wheel No. 3.

Modal analysis of grinding wheel natural vibrations

A computer simulation experiment was conducted using the finite element method in the *COMSOL Multiphysics* software environment to study natural frequencies and vibration modes. This software is widely used for engineering calculations worldwide and has proven effective in solving acoustic and vibration problems [16–20].

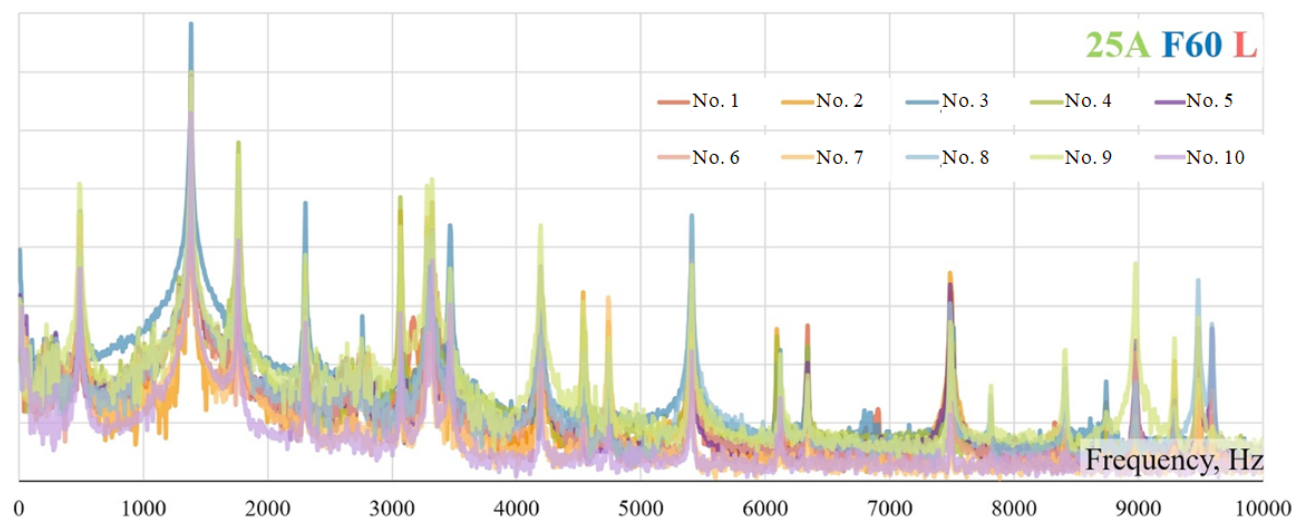


Fig. 3. Spectral composition of grinding wheel No.3 natural vibrations

A model of a grinding wheel was developed that allows parametric control over its geometry and elastic parameters. The following equation expresses the relationship between the natural frequencies of a grinding wheel's vibrations and its geometric dimensions, shape, and elastic parameters:

$$f_i = F_i(a, \nu) \sqrt{\frac{E}{\rho}}$$

where $F_i(a, \nu)$ is the shape factor, which depends on the body's geometrical dimensions and shape ($a = f(D, d, H)$), Poisson's ratio (ν), and the mode of oscillation.

The model parameters are summarized in Table 2.

Table 2

Grinding wheel model parameters

Symbol	Description
Geometrical model parameters	
D	GW outer diameter
d	GW inner diameter
H	GW height
Elastic parameters of model material	
ν	Poisson's ratio
E	Young's modulus
ρ	density

The calculation of eigenmodes and oscillation frequencies was carried out for each variant of the grinding wheel (GW) parameters – D , d , H , ν , E , and ρ – in order to determine the agreement with the experimentally obtained frequencies. The comparison is presented in the section “Comparison of experimental and calculated spectral compositions of grinding wheels”.

Results and Discussion

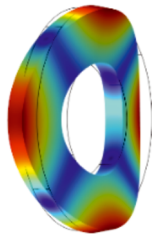
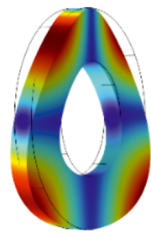
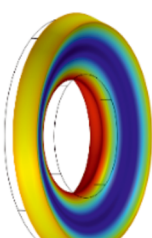
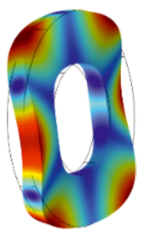
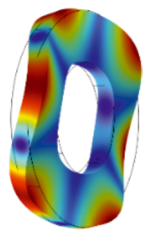
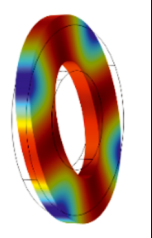
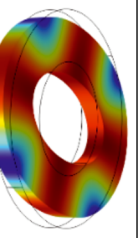
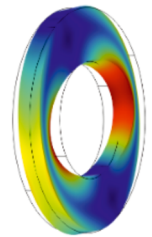
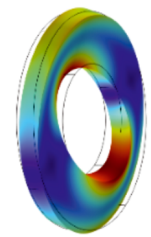
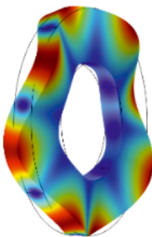
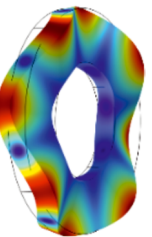
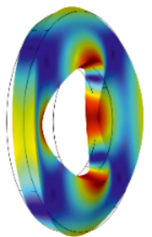
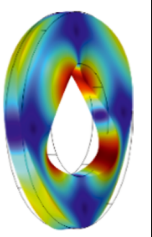
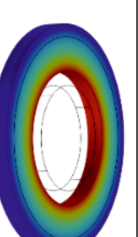
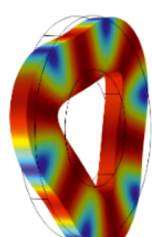
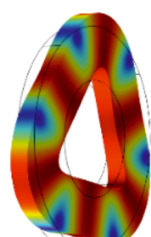
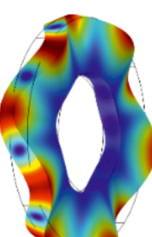
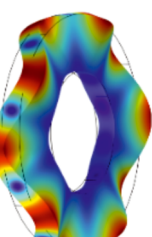
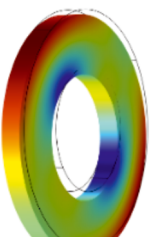
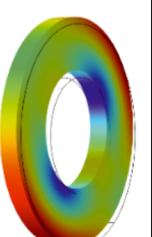
Eigenmodes of Grinding Wheel Vibration

Computer modeling has shown that the order in which eigenmodes of grinding wheel vibrations manifest remains unchanged over a wide range of values of ν , E , and ρ . The natural frequency values associated

with each mode vary depending on the values and combinations of the elastic parameters. The geometric parameters of grinding wheels have a decisive influence on the shapes of the modes, the sequence of their manifestation, and the corresponding frequencies. Table 3 summarizes the natural frequencies and their corresponding modes in the order of their manifestation for grinding wheel No. 3 – *GW 1 600×50×305 25A F60 L 7 V 50 2 class GOST R 52781-2007*.

Table 3

Occurrence order of grinding wheel natural oscillations modes*

No.	1	2	3	4	5	6	7
f , Hz	544.59	544.62	1187.6	1429.7	1429.71	1451.8	1451.81
Mode							
	Repeated modes			Repeated modes		Repeated modes	
No.	8	9	10	11	12	13	14
f , Hz	1983.3	1983.5	2555.5	2555.51	3440.4	3440.8	3503.5
Mode							
	Repeated modes		Repeated modes		Repeated modes		
No.	15	16	17	18	19	20	* – <i>GW 1 600×50×305 25A F60 L 7 V 50 2 class GOST P 52781-2007</i>
f , Hz	3508.8	3508.81	3850.0	3850.1	4503.5	4503.51	
Mode							
	Repeated modes		Repeated modes		Repeated modes		

Thus, a pair of the lowest modes are bending modes with two nodal diameters, f_1 and f_2 ($n = 2, s = 0$), followed by the bending mode f_3 with one nodal circle ($n = 0, s = 1$), called the “umbrella” mode in the literature [21]. This result agrees with the analytical calculations of vibration modes of grinding wheels by *B. A. Glagovsky* and *I. B. Moskovenko* [22]. In the study of vibrations of discs with a central axial hole, the letters n and s denote the number of nodal diameters and nodal circles, respectively. The grinding wheels considered in this study belong to this category.

The bending modes manifested in pairs f_4 and f_5 ($n = 3, s = 0$), f_{10} and f_{11} ($n = 4, s = 0$), and f_{17} and f_{18} ($n = 5, s = 0$) are similar and differ only in the number of nodal diameters. The pairs f_8 and f_9 ($n = 1$,

$s = 1$) and f_{12} and f_{13} ($n = 2, s = 1$) differ by the presence of a nodal circle and a different number of nodal diameters. The pairs f_6 and f_7 ($n = 2, s = 0$), f_{15} and f_{16} ($n = 3, s = 0$), f_{19} and f_{20} ($n = 1, s = 1$), and mode f_{14} ($n = 0, s = 1$) belong to the class of radial modes. These are characterized by tension-compression stresses, in which oscillations of microvolumes occur in the plane of the grinding wheel.

The peculiarity of the pairwise manifestation of modes with nodal diameters ($n \neq 0$) is emphasized. These modes are called multiple modes since they are vibration modes with close (or coinciding) natural frequencies, the same mode set but different orientations of nodal lines. Multiple modes appear in pairs and are characterized by the relative displacement of nodal diameters by some angle. Such modes occur in systems with a high degree of symmetry (e.g., circular discs, spherical shells, square plates). Their existence has been confirmed by both experimental studies and analytical calculations [23–26].

The smallest number of nodal lines, whether nodal diameters or nodal circles, are characteristic of the lowest modes, i.e., modes formed at the lowest frequencies characteristic of the “grinding wheel” system. As the number of nodal lines manifested in the vibrational motion of a particular mode increases, the frequency at which this mode occurs also increases. It is well known that the lowest modes are of primary importance in the overall dynamics of the vibrational process of an elastic solid. To describe the contribution of each mode, coefficients of modal participation and modal mass have been introduced. These coefficients will be discussed in more detail in “Modal Participation Coefficients”.

Modal participation coefficients

The participation coefficient indicates the relative contribution of each mode to the displacement or rotation of the system when excited in a specific direction and manner. Since no rotational modes or angular vibrations of the grinding wheel were identified in the computer simulations, the participation coefficients for rotational directions are not considered in this study.

Participation coefficients are calculated when it is necessary to determine the parameters of an external load that could potentially cause undesirable resonance in the system [27]. Such calculations make it possible to assess the significance of each mode participating in the vibration process. These modes are characterized by high vibration energies and sensitivity to specific types of loads. After identifying a significant mode in strength calculations, either the system’s operating modes should be changed or the design modernized to avoid undesirable consequences.

Fig. 4 shows the graph of participation coefficients of grinding wheel No. 3 – *GW 1 600×50×305 25A F60 L 7 V 50 2 class GOST R 52781-2007* – plotted along three coordinate axes. It demonstrates that the most significant eigenmodes of vibration of the grinding wheel are modes f_1 and f_2 , which are most pronounced in the X and Y directions. Regarding the Z axis, the largest contribution in this direction is made by the “umbrella” mode f_3 .

This mode will be used for acoustic monitoring of the grinding process. When applying boundary conditions, the displacement of the grinding wheel model is restricted – it is rigidly fixed along the seat diameter on the machine spindle. Additionally, a prestressing condition distributed over the volume of the grinding wheel is imposed, resulting from the centrifugal forces during rotation at a speed of 1,590 RPM.

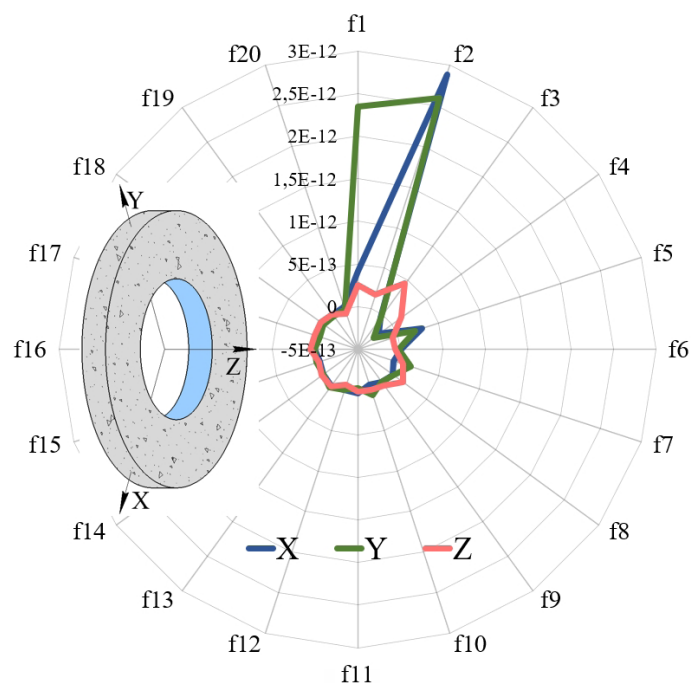


Fig. 4. Participation factors of the natural vibration modes of the grinding wheel along the coordinate axes

The order of eigenmodes' manifestation changes significantly as a result of calculating them under these specified boundary conditions. The bending mode with the highest values of modal participation coefficients and modal masses becomes the lowest and most significant mode, featuring a nodal circle coinciding with the end region — the “*umbrella*” mode. The participation of this mode in the overall dynamics of the grinding wheel vibrations is much greater (more than 30 times) than that of the others and, accordingly, it generates the most powerful acoustic wave.

Comparison of experimental and calculated spectral compositions of grinding wheels

In figs. 5, *a–k*, the black lines show the spectral compositions obtained experimentally using the method described in section “*Experimental study of natural vibrations of grinding wheels*”. These graphs illustrate the distribution of the natural frequencies of grinding wheels with the studied characteristics.

During computer modeling and the modal analysis process, the values of *Poisson's* ratio (ν) and *Young's* modulus (E) were adjusted to align the calculated frequency values (shown in the graphs as red vertical lines) with the experimental frequencies. The parametric optimization problem was solved using the fitting method. A perfect fit can only be achieved when the real geometric dimensions of the grinding wheels exactly match their modeled counterparts.

The frequencies coincide at a satisfactory level. The deviation of the calculated frequencies from the experimental values does not exceed 5 %. Consequently, the values of the integral elastic parameters, ν and E , were obtained for each grinding wheel considered:

- | | |
|--|---|
| 1. 25A F36 L – $\nu = 0.25$; $E = 51.25$ GPa; | 7. 25A F60 P – $\nu = 0.225$; $E = 54$ GPa; |
| 2. 25A F46 L – $\nu = 0.215$; $E = 46$ GPa; | 8. 25A F60 S – $\nu = 0.2$; $E = 67.5$ GPa; |
| 3. 25A F60 L – $\nu = 0.18$; $E = 41.5$ GPa; | 9. 14A F60 L – $\nu = 0.25$; $E = 41.2$ GPa; |
| 4. 25A F80 L – $\nu = 0.17$; $E = 40$ GPa; | 10. 64C F60 L – $\nu = 0.26$; $E = 43$ GPa; |
| 5. 25A F120 L – $\nu = 0.16$; $E = 45.5$ GPa; | 11. 92A F60 L – $\nu = 0.27$; $E = 53$ GPa. |
| 6. 25A F60 N – $\nu = 0.22$; $E = 48$ GPa; | |

Thus, although labor-intensive, this approach to determining ν and E is recognized as effective. The agreement between the calculated and experimental frequencies allows us to conclude that the simulated values of *Poisson's* ratio and *Young's* modulus of the grinding wheels correspond to those of their prototypes. Therefore, the main objective of this work has been achieved.

Currently, work is underway to develop a mathematical model of the sound pressure generated during grinding and a methodology for predicting the grinding wheel service life based on acoustic indices. This model requires taking into account the actual elasticity parameters of grinding wheels and establishing a relationship between these parameters and the wheels' characteristics.

The values of ν and E obtained during this study were used as parameters to develop a sound pressure model of the grinding process. Preliminary results show the model's qualitative agreement with, and adequacy to, the experimental acoustic data obtained during the grinding process study.

Dependence of integral elastic parameters on grinding wheel characteristics

The study of grinding wheels No. 1, No. 2, No. 3, No. 4, and No. 5 determined the influence of abrasive grain size on the elastic parameters, ν and E . *Poisson's* ratio decreases as the abrasive grain size decreases. *Young's* modulus decreases until the grain size reaches 0.2 mm; thereafter, the trend reverses and begins to increase. However, there is insufficient data to conclude whether the increase in *Young's* modulus will continue as the grain size is further reduced.

Fig. 6 shows graphs reflecting this dependence in terms of granularity versus *Poisson's* ratio and granularity versus *Young's* modulus. Next, regression equations and curves were obtained using *MS Excel*. The regression curves constructed from the experimental data are expressed by second-degree polynomial

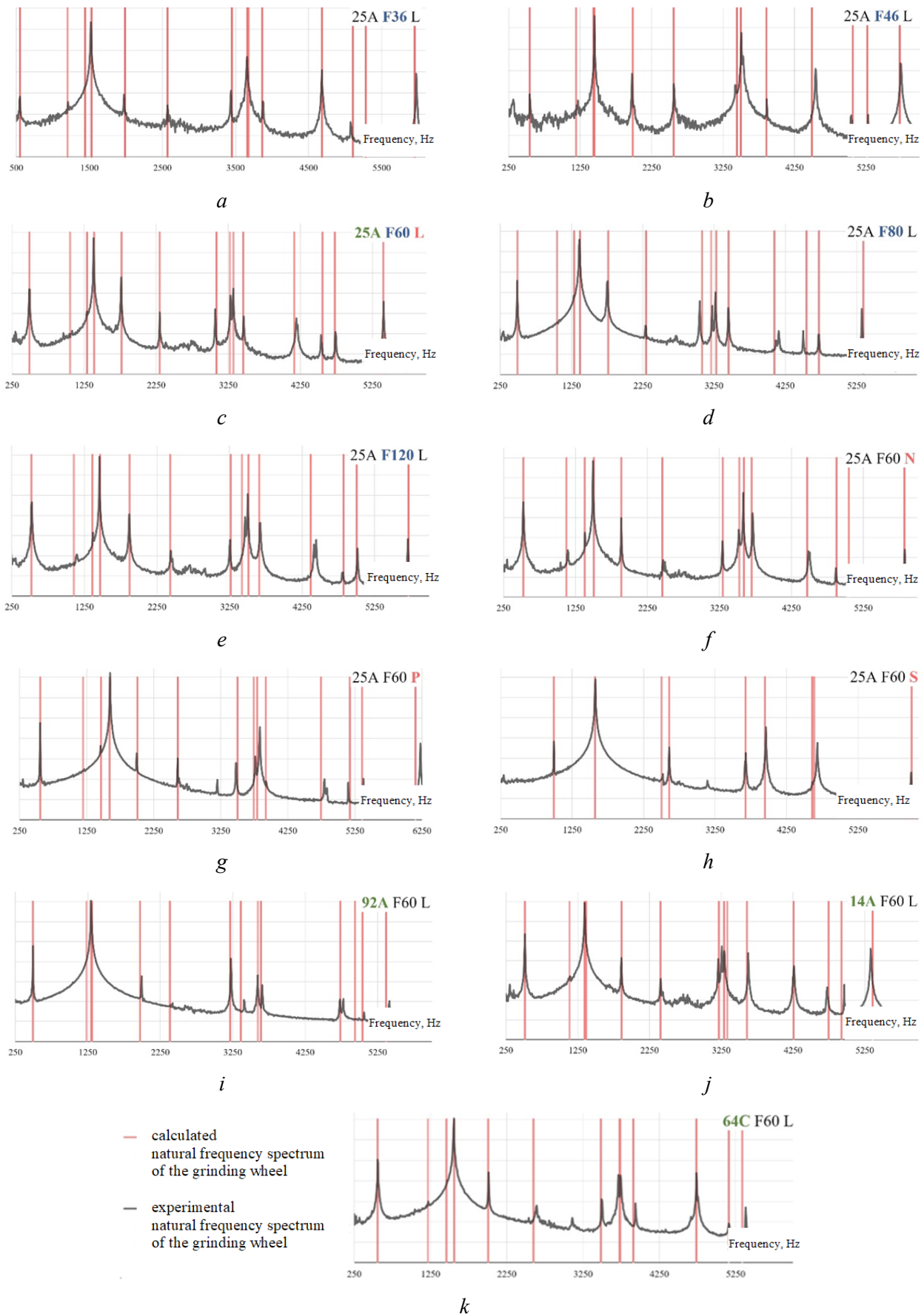


Fig. 5. Comparison of empirical and calculated spectral compositions of natural vibrations of grinding wheel: *a* – 25A F36 L; *b* – 25A F46 L; *c* – 25A F60 L; *d* – 25A F80 L; *e* – 25A F120 L; *f* – 25A F60 N; *g* – 25A F60 P; *h* – 25A F60 S; *i* – 14A F60 L; *j* – 92A F60 L; *k* – 64C F60

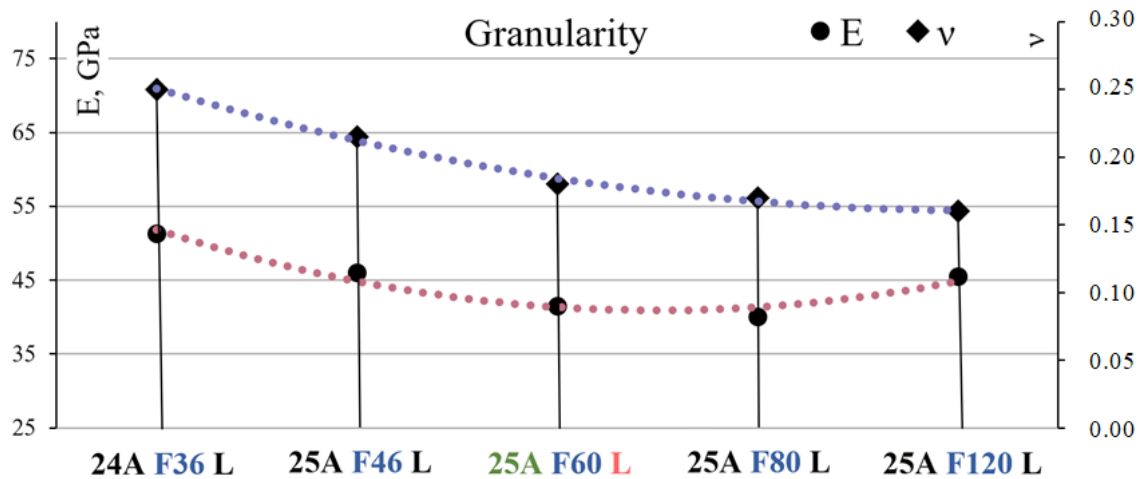


Fig. 6. Influence of grinding wheel grit on the value of *Poisson's ratio* and *Young's modulus*

dependencies with approximation reliability levels of $R^2 = 0.949$ for the *Young's modulus* dependency curve and $R^2 = 0.993$ for the *Poisson's ratio* dependency curve. This indicates a strong correlation between the values of ν , E and the grain size factor.

$$\nu = 0.0054 \cdot x^2 - 0.054 \cdot x + 0.3;$$

$$E = 1.75 \cdot x^2 - 12.25 \cdot x + 62.35.$$

It should be noted that the obtained regression relations are not claimed to be universal and can only be applied under the conditions in which they were derived. For instance, the values of ν and E can be determined for a grinding wheel with the following characteristics: an abrasive of white electrocorundum with a hardness grade of L and an average structure number of 6 on a ceramic bond. For a grinding wheel with a grit size of $F100$ (grit size ranging from 0.15 to 0.11 mm), the values of *Poisson's ratio* and *Young's modulus* are 0.164 and 42.66 GPa, respectively.

Similarly, the effect of hardness on the elastic performance of grinding wheels has been established. An increase in grinding wheel hardness results in higher values of *Young's modulus*. *Young's modulus* characterizes the stiffness of the system and its ability to resist elastic deformation. This is reflected in the study of natural vibrations of a solid body. Grinding wheels with higher E values exhibit a shift of natural frequencies toward the high-frequency range (see Fig. 5).

The change in hardness of grinding wheels with the same structure is due to the redistribution of the proportions of the main components: grain, bond, and pores. An increase in hardness is promoted by a decrease in pore volume and an increase in bond volume. Therefore, it can be concluded that there is a positive correlation between hardness and stiffness, or between the characteristics of plastic and elastic deformation of the grinding wheel, as expressed by *Young's modulus*.

Poisson's ratio increases with hardness in the interval from L to P . After reaching a maximum value of 0.23 , it begins to decrease. See fig. 7 for the graphs.

The obtained regression dependencies have approximation confidence levels close to unity ($R^2 = 0.9913$ for the *Young's modulus* curve and $R^2 = 0.999$ for the *Poisson's ratio* curve). Therefore, there is a strong correlation between the values of ν , E , and the hardness factor.

$$\nu = -0.0162 \cdot x^2 + 0.0877 \cdot x + 0.109;$$

$$E = 1.75 \cdot x^2 - 0.35 \cdot x + 40.5.$$

These empirical regression models can be used to determine the values of ν and E for white electrocorundum grinding wheels with an $F60$ grain size and medium structure on a ceramic bond for several hardness grades: K , M , O , R , and T :

- $25A F60 K$ has values $\nu = 0.148$; $E = 40.76$ GPa;
- $25A F60 M$ has values $\nu = 0.200$; $E = 43.91$ GPa;

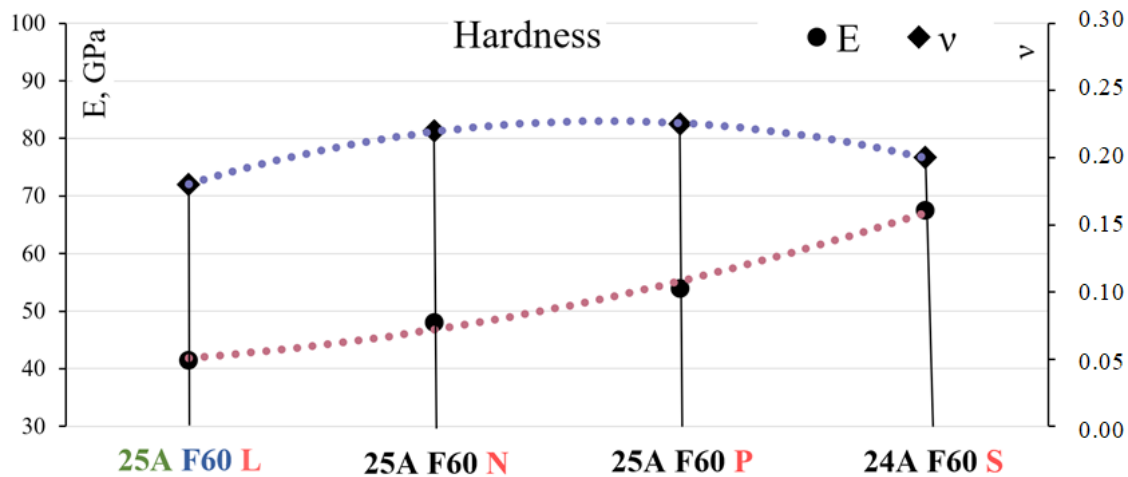


Fig. 7. Influence of grinding wheel hardness on the value of *Poisson's ratio* and *Young's modulus*

- 25A F60 O has values $\nu = 0.227$; $E = 50.56$ GPa;
- 25A F60 R has values $\nu = 0.217$; $E = 60.713$ GPa;
- 25A F60 T has values $\nu = 0.175$; $E = 74.36$ GPa.

Values of *Poisson's ratio* and *Young's modulus* were also obtained for grinding wheels made of normal electrocorundum, white electrocorundum, chromotitanium electrocorundum, and green silicon carbide (see fig. 8). Since the abrasive material of the grinding wheel cannot be quantified, regression analysis and the development of empirical relationships are not applicable in this case, unlike in the study of the effect of grain size and hardness on the elastic parameters of the tool. The values of ν and E in fig. 8 do not permit further applications or insights beyond what is obtained directly.

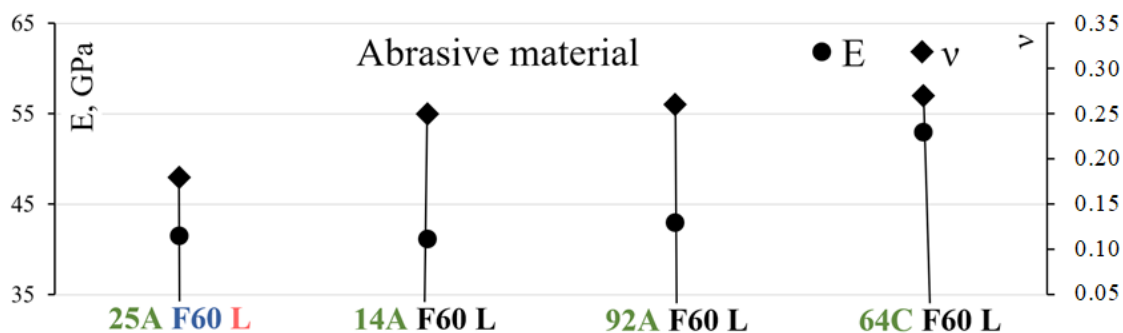


Fig. 8. Influence of abrasive material on the value *Poisson's ratio* and *Young's modulus*

Conclusion

1. The order of appearance of the eigenmodes of grinding wheel vibrations remains unchanged over a wide range of ν and E values. The lowest eigenmodes used for acoustic monitoring of grinding wheels are a pair of bending modes f_1, f_2 ($n = 2, s = 0$) and the bending mode f_3 ($n = 0, s = 1$).

2. In the absence of boundary conditions, modes f_1 and f_2 ($n = 2, s = 0$) contribute most significantly to the dynamics of grinding wheel vibrations along the X and Y coordinate axes. In the Z direction, the largest contribution is made by eigenmode f_3 ($n = 0, s = 1$); however, this contribution is much smaller than that of f_1 and f_2 .

3. The values of *Poisson's ratio* and *Young's modulus* for the studied grinding wheels were determined by correlating the experimental and calculated spectral compositions of the natural frequency distributions. The values vary within the following ranges: $0.16 < \nu < 0.27$ and $40 \text{ GPa} < E < 67.5 \text{ GPa}$. Grinding wheels with significantly different characteristics (e.g., 25A F80 L and 25A F60 S) may have slightly different

Poisson's ratio values ($\nu = 0.17$ and $\nu = 0.2$, respectively). This underscores the importance of accurately determining the integral elastic parameters of the tool to correctly model the sound pressure generated during the grinding process. Even a slight error in determining *Poisson's* ratio can lead to discrepancies between the modeled wheel's characteristics and its actual behavior.

4. Empirical regression dependencies of the integral elastic parameters of grinding wheels on abrasive grain size and hardness have been obtained with a high degree of reliability and accuracy.

References

1. Ardashev D.V., Zhukov A.S. Issledovanie spektral'nogo sostava svobodnykh akusticheskikh kolebaniy shlifoval'nykh krugov na keramicheskoi svyazke [Research of spectral composition of natural acoustic vibrations of ceramic-bonded grinding wheels]. *Metalloobrabotka = Metalworking*, 2023, no. 1 (133), pp. 3–20. DOI: 10.25960/mo.2023.1.3. (In Russian).
2. Ardashev D.V., Zhukov A.S. Investigation of the relationship between the cutting ability of the tool and the acoustic signal parameters during profile grinding. *Obrabotka metallov (tekhnologiya, oborudovanie, instrumenty) = Metal Working and Material Science*, 2022, vol. 24, no. 4, pp. 64–83. DOI: 10.17212/1994-6309-2022-24.4-64-83. (In Russian).
3. Li C., Song Z., Huang X., Zhao H., Jiang X., Mao X. Analysis of dynamic characteristics for machine tools based on dynamic stiffness sensitivity. *Processes*, 2021, vol. 9 (12), art. 2260, pp. 1–16. DOI: 10.3390/pr9122260.
4. Xiao H., Hu X., Luo S., Li W. Developing and testing the proto type structure for micro tool fabrication. *Machines*, 2022, vol. 10 (10), art. 938, pp. 1–21. DOI: 10.3390/machines10100938.
5. Lin C.-Y., Luh Y.-P., Lin W.-Z., Lin B.-C., Hung J.-P. Modeling the static and dynamic behaviors of a large heavy-duty lathe machine under rated loads. *Computation*, 2022, vol. 10 (12), art. 207, pp. 1–18. DOI: 10.3390/computation10120207.
6. Chan T.-C., Chang C.-C., Ullah A., Lin H.-H. Study on kinematic structure performance and machining characteristics of 3-axis machining center. *Applied Sciences*, 2023, vol. 13 (8), art. 4742, pp. 1–29. DOI: 10.3390/app13084742.
7. Behera R., Chan T.-C., Yang J.-S. Innovative structural optimization and dynamic performance enhancement of high-precision five-axis machine tools. *Journal of Manufacturing and Materials Processing*, 2024, vol. 8 (4), art. 181, pp. 1–25. DOI: 10.3390/jmmp8040181.
8. Vázquez C.R., Guajardo-Cuéllar A. Prediction of vertical vibrations of a CNC router type geometry. *Applied Sciences*, 2024, vol. 14 (2), art. 621, pp. 1–23. DOI: 10.3390/app14020621.
9. Chi Y., Dai W., Lu Z., Wang M., Zhao Y. Real-time estimation for cutting tool wear based on modal analysis of monitored signals. *Applied Sciences*, 2018, vol. 8 (5), art. 708, pp. 1–13. DOI: 10.3390/app8050708.
10. Nie W., Zheng M., Xu S., Liu Y., Yu H. Stability analysis and structure optimization of unequal-pitch end mills. *Materials*, 2021, vol. 14 (22), art. 7003, pp. 1–13. DOI: 10.3390/ma14227003.
11. Wang J., Qian J., Huang K., Shang Z., Yu J. Chatter and surface waviness analysis in Oerlikon face hobbing of spiral bevel gears. *Aerospace*, 2024, vol. 11 (7), art. 535, pp. 1–25. DOI: 10.3390/aerospace11070535.
12. Mladjenovic C., Monkova K., Zivkovic A., Knezev M., Marinkovic D., Ilic V. Experimental identification of milling process damping and its application in stability lobe diagrams. *Machines*, 2025, vol. 13 (2), art. 96, pp. 1–24. DOI: 10.3390/machines13020096.
13. Nowakowski L., Blasiak S., Skrzyniarz M., Rolek J. Experimental-analytical method for determining the dynamic coefficients of turning tools. *Materials*, 2025, vol. 18 (3), art. 563, pp. 1–15. DOI: 10.3390/ma18030563.
14. Ovchinnikov A.I. Materialy dlya abrazivnogo instrumenta. Obzor [Materials for an abrasive tool. Review]. *Nauka i obrazovanie = Science and Education*, 2013, no. 7, pp. 41–68, DOI: 10.7463/0713.0577449. (In Russian).
15. Abyzov A.M. Oksid alyuminiya i alyumooksidnaya keramika (Obzor). Ch. 1. Svoistva Al_2O_3 i promyshlennoe proizvodstvo dispersnogo Al_2O_3 [Aluminum oxide and alumina ceramics (Review). Part 1. Properties of Al_2O_3 and industrial production of dispersed Al_2O_3]. *Novye ognepupory = New Refractories*, 2019, no. 1, pp. 16–23. DOI: 10.17073/1683-4518-2019-1-16-23.
16. Zhang H., Jiao F., Niu Y., Li C., Zhang Z., Tong J. Design and experimental study of longitudinal-torsional composite ultrasonic internal grinding horn. *Micromachines*, 2023, vol. 14 (11), art. 2056, pp. 1–17. DOI: 10.3390/mi14112056.
17. Li F., Chen Y., Zhu D. Revealing the sound transmission loss capacities of sandwich metamaterials with re-entrant negative Poisson's ratio configuration. *Materials*, 2023, vol. 16 (17), art. 5928, pp. 2–21. DOI: 10.3390/ma16175928.



18. Zhang Y., Tu H., Wang Y., Xu G., Gao D. A normal mode model based on the spectral element method for simulating horizontally layered acoustic waveguides. *Journal of Marine Science and Engineering*, 2024, vol. 12 (9), art. 1499, pp. 1–16. DOI: 10.3390/jmse12091499.
19. Wang Y., Zhao D., Jia Y., Wang S., Du Y., Li H., Zhang B. Acoustic sensors for monitoring and localizing partial discharge signals in oil-immersed transformers under array configuration. *Sensors*, 2024, vol. 24 (14), art. 4704, pp. 1–24. DOI: 10.3390/s24144704.
20. Dai Y., Li S., Feng M., Chen B., Qiao J. Fundamental study of phased array ultrasonic cavitation abrasive flow polishing titanium alloy tubes. *Materials*, 2024, vol. 17 (21), art. 5185, pp. 1–19. DOI: 10.3390/ma17215185.
21. Yuganov V.S. *Ispol'zovanie nizkochastotnykh akusticheskikh kolebaniy dlya tekushchego kontrolya protsessy shlifovaniya*. Diss. kand. tekhn. nauk [Use of low-frequency acoustic oscillations for current control of the grinding process. PhD eng. sci. diss.]. Ul'yanskovsk, 1999. 198 p.
22. Glagovskii B.A., Moskovenko I.B. *Nizkochastotnye akusticheskie metody kontrolya v mashinostroenii* [Low-frequency acoustic control methods in mechanical engineering]. Leningrad, Mashinostroenie Publ., 1977. 203 p.
23. Smirnov V.A., Nanasov M.P. [Calculation of frequencies and forms of vibrations of a round plate]. *Perspektivy razvitiya stroitel'nykh konstruktov* [Prospects of building structures development]. Materials of scientific-practical conference. Leningrad, LDNTP Publ., 1987, pp. 68–72. (In Russian).
24. Ivanov V.P. *Kolebaniya rabochikh koles turbomashin* [Vibrations of turbomachine impellers]. Moscow, Mashinostroenie Publ., 1983. 224 p.
25. Makaeva R.Kh., Karimov A.Kh., Tsareva A.M. Issledovanie rezonansnykh kolebaniy diskov s primeneniem golograficheskoi interferometrii [Research of resonance vibrations of discs with application of holographic interferometry]. *Vestnik dvigatelestroeniya = Herald of Aeroenginebuilding*, 2012, no. 2, pp. 161–165.
26. Tsareva A.M. *Eksperimental'no-raschetnyi metod opredeleniya rezonansnykh chastot i form kolebaniy detalei tipa diskov s primeneniem golograficheskoi interferometrii*. Avtoref. diss. kand. tekhn. nauk [Experimental-calculation method of determination of resonance frequencies and vibration forms of disc-type parts using holographic interferometry. Author's abstract of PhD eng. sci. diss.]. Kazan', 2007. 20 p.
27. Vázquez M., López V., Campos R., Cadenas E., Marin P. Structural and modal analysis of a small wind turbine blade considering composite material and the IEC 61400-2 standard. *Energies*, 2025, vol. 18 (3), art. 566, pp. 1–26. DOI: 10.3390/en18030566.

Conflicts of Interest

The authors declare no conflict of interest.

© 2025 The Authors. Published by Novosibirsk State Technical University. This is an open access article under the CC BY license (<http://creativecommons.org/licenses/by/4.0>).

